

## THREE-DIMENSIONAL FINITE ELEMENT ANALYSIS OF HUMAN FOOT DURING HEEL RISE: ROLE OF THE GASTROCNEMIUS-SOLEUS (G-S) MUSCLE

Wenming Chen and Peter Vee Sin Lee

Department of Mechanical Engineering, University of Melbourne, Australia

Geometric positioning of the foot and transfer of plantar loads can be adversely affected when muscular control in gastrocnemius-soleus (G-S) complex is abnormal. This study aims to develop a 3-D musculoskeletal finite element (FE) model of the foot to quantify the precise role of the G-S complex in biomechanical behavior of the foot. Movements of the ankle and metatarsophalangeal joints, as well as forefoot plantar pressure peaks and pressure distribution under the metatarsal heads (MTHs) were all found to be extremely sensitive to reduction in the muscle load in the G-S complex. The findings may provide clinicians with knowledge to understand the underlying mechanism for relieving pain, injury or other structural deformities under metatarsal areas in patients who suffer from G-S muscle contracture.

**KEY WORDS:** foot, planter pressure, flexor muscle, metatarsal head.

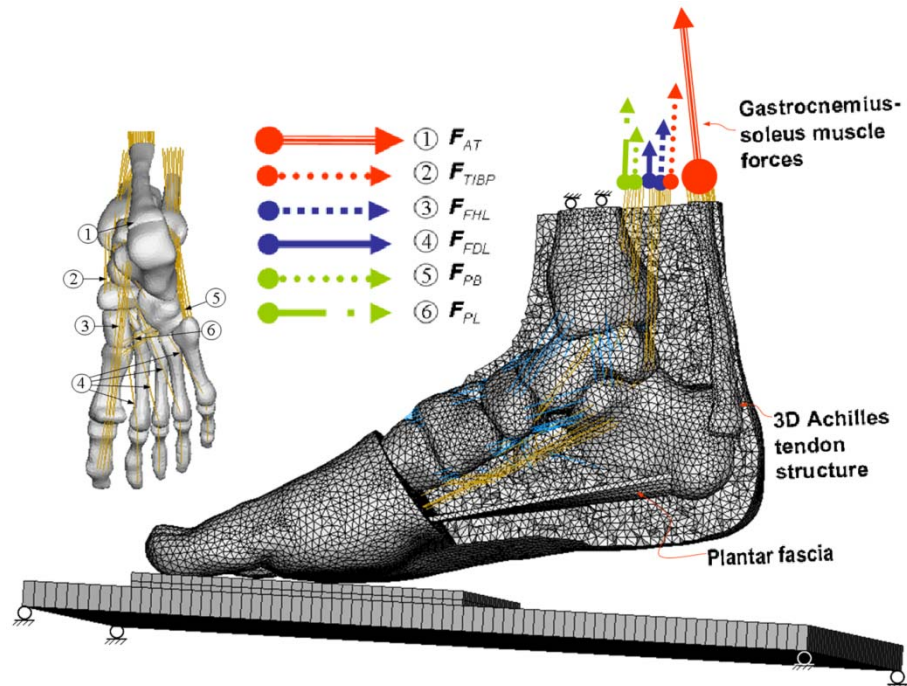
**INTRODUCTION:** The gastrocnemius-soleus (G-S) complex associated with the Achilles tendon is the most dominant extrinsic plantar flexor. Various studies using cadaveric foot models have established the important biomechanical roles and relationships among the Achilles tendon, plantar fascia and metatarsophalangeal (MTP) joints, earlier described as the Windlass mechanism (Erdemir, Hamel, Fauth, Piazza, & Sharkey, 2004). With the foot stabilized by flexor muscles upon heel rise, substantial dynamic ground reaction forces (GRF) are imposed on the forefoot plantar surface, thereby generating localized stresses, particularly underneath the metatarsal heads (MTHs). The potentially harmful stresses only last for a short-dwelling time in a normal foot due to optimal muscles forces and activation patterns. However, in the case of equinus contracture, normal muscle activations in the G-S complex may be compromised (Lin, Lee, & Wapner, 1996). The contractured G-S muscle consistently exerts tension through the Achilles tendon, resulting in an earlier Windlass effect accompanied by premature heel rise, and the maintenance of this abnormal posture throughout the whole stance phase of walking. Many believed that this leads to prolonged and high-magnitude forefoot loading exposure, which may induce pain, injury or other structural deformities in these areas over time, such as metatarsalgia and forefoot plantar skin injury (Bowers & Castro, 2007). Manipulation of the muscle force in the G-S complex via surgical intervention, such as tendo-Achilles lengthening, can negate the 'abnormal' Windlass mechanism associated with G-S muscle contracture, and appears effective in restoring normal forefoot load transfer by relieving the abnormally high stresses under the MTHs. In the case of a diabetic foot, tendon Achilles lengthening has been used to help facilitates ulcers' healing. In contrast, Orendurff et al. (2006), showed that equinus contracture accounts for only a small amount of the increased forefoot plantar pressure. There is still a dearth of information on the precise role the G-S complex during gait.

The aim of this study is to investigate the adaptive changes of the foot mechanism (ankle and MTP joint movements and forefoot load), in response to force variations generated by the G-S muscle complex. This is done by means of a musculoskeletal finite element (FE) model of the foot. The quantitative analysis using a FE foot model may help explain the etiology of many foot and ankle disorders associated with G-S contracture and treatment benefits such as tendo-Achilles lengthening. This study also addresses some of the significant limitations of previous FE models due to the absence of muscle actuation and stabilization.

**METHODS:** A three dimensional (3-D) FE model of the human foot was created, by refining a previous soft-tissue-skeletal model to accommodate muscle attachments as shown in Figure 1. Six major extrinsic plantar flexors were included. To model the G-S complex, a 3-D

geometry of the Achilles tendon was constructed and incorporated into the extreme posterior of the calcaneus. This facilitates application of G-S muscle forces through the Achilles tendon-bone junction, and ensure more realistic muscle load transfer compared to the previous model, which only employed nodal points to apply such forces. The long tendons of the other five muscles (Figure 1) were also incorporated into the model, at their corresponding anatomical attachment sites. This was done using bar elements based on straight-line approximation, i.e. several bar elements strung together to represent the actual tendon trajectory inside the foot. Surface-to-surface contact elements with no friction simulated the relative articulating movements between joint surfaces, the contact elements allowed the bones to slide over one another with the only constraint governed by the congruent surfaces. The material properties of various tissue components were obtained from our previous model (Chen, Lee, & Lee, 2010).

**Figure 12: Finite element model of muscular foot and ankle complex, incorporating internal soft tissue, skeletal structures, ligaments, plantar fascia, and musculotendinous units. (Muscle forces:  $F_{AT}$  = Gastrocnemius-soleus complex,  $F_{TIBP}$  = Tibialis posterior,  $F_{FHL}$  = Flexor hallucis longus,  $F_{FDL}$  = Flexor digitorum longus,  $F_{PB}$  = Peroneus brevis, and  $F_{PL}$  = Peroneus longus.)**



The instant the forefoot force reaches a peak (i.e. second peak of walking GRF) was chosen for simulation. At the commencement of simulation, the foot pose relative to the ground was adjusted so that the second metatarsal shaft was angled at approximately 25 degrees to the horizontal to reflect mean forefoot orientation in the sagittal plane (i.e. the main loading plane) at push-off. The tibia, fibula and the superior surfaces of the soft tissue were fully constrained. Application of extrinsic muscle forces was simulated via force vectors in axial alignment with the tendons attached (Figure 1). A targeted maximum vertical GRF, approximating the second walking GRF peak, was generated solely by contracting the plantar flexors at the prescribed kinematic configuration. This loading protocol mimicked the manipulations in the cadaveric study conducted by Sharkey et al. (1995). The initial configurations of the metatarsals were affected slightly because of considerable deformation of the plantar soft tissues. The simulation and solution converged with the 2nd metatarsal shaft oriented at 26.8 degrees to the horizontal. The corresponding total muscle force (TMF) was computed and the forces in individual muscles are assumed to be proportional to their physiological cross-sectional areas (PCSA); i.e. the  $i$ th muscle force (MF) is given by:

$$MF_i = \frac{PCSA_i}{\sum_{j=1}^6 PCSA_j} \bullet TMF \quad (i = 1,2,3,4,5,6)$$

To study the effects of varying the G-S complex muscle force (denoted as  $F_{AT}$ ), a multi-step analysis procedure was adopted. The initially loaded baseline model served as the reference for subsequent analysis. The maximum  $F_{AT}$  was reduced in steps of 10% down to 60% of the original, to simulate reduced muscle effectiveness of the G-S complex (Table 1). The maximum GRF were maintained at the foot-supporting surface, and the ground was allowed to move in the vertical direction. The stresses and deformations of the baseline model were updated in sequential steps to determine the consequences of decreasing the  $F_{AT}$ .

**Table 1: The input forces in the muscles applied through the nodes connected to tendon elements to drive the finite element foot model.**

	$i^{\text{th}}$ muscle		Muscle forces		No. of nodes
#1	Gastrocnemius Soleus	$F_{AT}$	100%	1620N	30
			90%	1458N	
			80%	1296N	
			70%	1134N	
			60%	972N	
#2	Tibialis posterior	$F_{TIBP}$	100%	267N	5
#3	Flexor hallucis longus	$F_{FHL}$	100%	130N	4
#4	Flexor digitorum longus	$F_{FDL}$	100%	81N	5
#5	Peroneus brevis	$F_{PB}$	100%	91N	5
#6	Peroneus longus	$F_{PL}$	100%	193N	5

**RESULTS:** With full muscular loads applied, the baseline foot model was successfully solved for a typical geometry at heel rise, with the ankle and MTP joints maintained at plantar-flexed and extended configurations, respectively. The predicted joint angles were significantly affected by variations (i.e. reduction) in  $F_{AT}$ . With decreased muscle stabilization, the ankle joint rotates by  $8.81^\circ$  from plantarflexion ( $6.05^\circ$ ) to dorsiflexion ( $-2.76^\circ$ ). This was coupled by MTP joint movements; an average decrease from  $-9.04^\circ$  to  $-4.39^\circ$  in joint extension was found (Table 2).

**Table 2: Relationship between gastrocnemius-soleus muscle forces ( $F_{AT}$ ) and joint angles for the ankle and MTP. ('-' means dorsiflexion).**

% $F_{AT}$	100	90	80	70	60
Ankle (°)	$6.05^\circ$	$3.48^\circ$	$0.06^\circ$	$-1.04^\circ$	$-2.76^\circ$
MTP	$-9.04^\circ$	$-7.8^\circ$	$-6.25^\circ$	$-5.45^\circ$	$-4.39^\circ$

The effect of a decreased  $F_{AT}$  on the forefoot plantar load distribution is marginal. In terms of plantar pressure, the location of the highest pressure predicted shifted from the 2<sup>nd</sup> MTH to the 1<sup>st</sup>, 3<sup>rd</sup>, and 4<sup>th</sup> MTHs. This was accompanied by an expansion of the contact area from the metatarsal region to the distal side (i.e. close to mid-foot region), resulting in a decrease of the overall peak plantar pressure from 321.1 to 261.7 kPa. Variations of the local pressure peaks at individual MTHs are site-specific. The most prominent relief of focal stresses was found at areas underneath the 2<sup>nd</sup> and 3<sup>rd</sup> MTHs. Peak pressures there were reduced by 20.1% and 14.6%, respectively. Peak pressure changes under the 4<sup>th</sup> MTH were negligible. There was 6.9% increase in the 1<sup>st</sup> MTH peak pressure for the initial 20% reduction in the  $F_{AT}$ , but no further changes thereafter. The peak pressure at the 5<sup>th</sup> MTH was almost doubled when the  $F_{AT}$  was decreased to 60% of the original, although the absolute stress values remained low.

**DISCUSSION:** This study is designed to investigate how the G-S muscle complex contributes to the weight-bearing function of the foot. When muscle forces generated by the G-S complex was reduced to 60% of the original (from 1,620N to 972N in a step-wise manner), dorsal-directed rotation of the ankle was increased and MTP joint extension was reduced. In addition, the changes in the G-S muscle complex also lead to a re-arrangements of the internal joints of the foot and the subsequent plantar pressures redistributions. The present study shows that the overall peak plantar pressure decreases by 22.7% in response to the prescribed reductions in the  $F_{AT}$ . Although these changes appear associated with increased ankle dorsiflexion, the actual cause could be the smaller inclination angle of the metatarsals to the horizontal, leading to more even load distribution among the five foot rays. Such plantar load redistribution could be extremely sensitive, since the average angular changes at MTP joints were only less than 5°. This is also evident in the model's solution, which showed that the plantar-directed displacements of the MTHs were generally decreased by about 42%. A similar reason has also been suggested by D'Ambrogi et al. (2005), that releasing the load on the Achilles tendon may alleviate the risk of cavoid foot formation (a common foot deformity with plantar flexion of the metatarsals that frequently occurs in diabetic patients). This again, highlights the importance of Achilles tendon loading in forefoot weight-bearing, which is closely related to stance-phase placement of the foot.

**CONCLUSION:** This investigation predicted alterations in the biomechanical behavior of the foot mechanism resulting from variations of muscle strength in the G-S complex. The stance-phase placement of the foot was found to be extremely sensitive to changes in G-S muscle forces, which leads to forefoot plantar pressure redistribution. The findings provide clinicians with knowledge to understand the underlying mechanism for relieving pain, injury or other structural deformities under plantar metatarsal areas in patients who suffer from G-S muscle contracture.

#### REFERENCES:

- Erdemir, A., Hamel, A. J., Fauth, A. R., Piazza, S. J. & Sharkey, N. A., (2004). Dynamic loading of the plantar aponeurosis in walking. *Journal of Bone and Joint Surgery* 86-A, 546-552.
- Lin, S. S., Lee, T. H. & Wapner, K. L., (1996). Plantar forefoot ulceration with equinus deformity of the ankle in diabetic patients: the effect of tendo-Achilles lengthening and total contact casting. *Orthopedics* 19, 465-475.
- Bowers, A. L. & Castro, M. D., (2007). The mechanics behind the image: foot and ankle pathology associated with gastrocnemius contracture. *Seminars in Musculoskeletal Radiology*, 11, 83-90.
- Orendurff, M. S., Rohr, E. S., Sangeorzan, B. J., Weaver, K. & Czerniecki, J. M., (2006). An equinus deformity of the ankle accounts for only a small amount of the increased forefoot plantar pressure in patients with diabetes. *Journal of Bone and Joint Surgery, British Volume* 88, 65-68.
- Chen, W.M., Lee, T., & Lee, P.V., (2010). Effects of internal stress concentrations in plantar soft-tissue-A preliminary three-dimensional finite element analysis. *Medical Engineering & Physics* 32, 324-331.
- Sharkey, N. A., Ferris, L., Smith, T. S. & Matthews, D. K., (1995). Strain and loading of the second metatarsal during heel-lift. *Journal of Bone and Joint Surgery* 77, 1050-1057.
- D'Ambrogi, E., Giacomozzi, C., Macellari, V. & Uccioli, L., (2005). Abnormal foot function in diabetic patients: the altered onset of Windlass mechanism. *Diabetic Medicine* 22, 1713-1719.